

The Carbonylation Reaction of $\text{CH}_3\text{Co}(\text{CO})_4$: A Detailed Density Functional Study

Sor Koon Goh and Dennis S. Marynick*

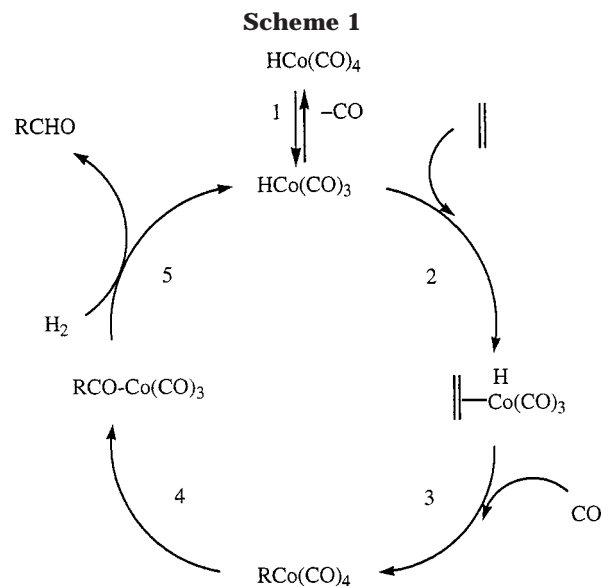
Department of Chemistry and Biochemistry, University of Texas at Arlington,
Arlington, Texas 76019-0065

Received January 14, 2002

The alkyl group migration reaction $\text{CH}_3\text{Co}(\text{CO})_4 \rightarrow \text{CH}_3(\text{CO})\text{Co}(\text{CO})_3$ and the carbonyl association reaction $\text{CH}_3(\text{CO})\text{Co}(\text{CO})_3 + \text{CO} \rightarrow \text{CH}_3(\text{CO})\text{Co}(\text{CO})_4$ have been thoroughly investigated via density functional theory techniques. In the migratory insertion reaction, two stable 16-electron acyl intermediates have been located on the B3LYP potential energy surface. Both species have the carbons of the acyl groups in the axial position. One of the intermediates is stabilized by the formation of an agostic interaction to the formally vacant site of the trigonal bipyramid, and the other is stabilized by the acyl oxygen adopting an η^2 coordination geometry. The transition states between all the intermediates, as well as several internal rotation processes, have been located. An interesting feature of this reaction is that alkyl group migration is accompanied by a simultaneous twist of the alkyl group into the equatorial plane of the original trigonal bipyramid, and therefore the reaction does not take place on a C_s symmetry potential energy surface. The transition states for CO association with each intermediate have also been characterized. Our calculations indicate that the formation of the acyl intermediates proceeds via methyl migration and that thermal carbonylation of the agostically stabilized and the η^2 stabilized intermediates is probably competitive.

Introduction

The conversion of olefins and synthesis gas ($\text{CO} + \text{H}_2$) into aldehydes (known as the hydroformylation reaction) using low-valence cobalt or rhodium as catalyst has become an important industrial process since it was first introduced in 1938 by Roelen.¹ The widely accepted mechanism (see Scheme 1) for the hydroformylation reaction with $\text{HCo}(\text{CO})_4$ as a precatalyst is due to Heck and Breslow.² On the basis of the investigation of the products isolated from the hydroformylation of olefins, Heck and Breslow proposed the following five-step mechanism. The first step involves the dissociation of a CO ligand to form a catalytically active $\text{HCo}(\text{CO})_3$ species. The existence of $\text{HCo}(\text{CO})_3$ has been demonstrated with matrix isolation techniques,³ and Ungváry and Markó⁴ also showed that $\text{HCo}(\text{CO})_4$ is about 0.3% dissociated to $\text{HCo}(\text{CO})_3$ at room temperature. In the second step, the unsaturated 16-electron $\text{HCo}(\text{CO})_3$ species forms a π complex with the olefin. In the third step, $\text{RCo}(\text{CO})_4$ (where R = alkyl) is produced by migratory insertion of the olefin into the Co–H bond and subsequent coordination of CO. Step four involves the formation of the 16-electron acyl complex $\text{R}(\text{CO})\text{Co}(\text{CO})_3$ through the intramolecular migration of the alkyl group to a cis CO ligand. Finally, oxidative addition of H_2 to the acyl complex, followed by reductive



elimination of aldehyde and the recovery of $\text{HCo}(\text{CO})_3$, completes the catalytic cycle.

While the above reactions have been well studied in many respects,⁵ experimental determination of the structures of all possible intermediates and transition states has not been possible. There have been several theoretical studies^{6–10} on this catalytic cycle. In a

(1) Roelen, O. (Ruhrchemie AG). D.G.B. 849 458 1938; *Chem. Zentr.* **1953**, 927.

(2) Heck, F.; Breslow, D. S. *J. Am. Chem. Soc.* **1961**, *83*, 4023.

(3) Wermer, P.; Ault, B. S.; Orchin, M. *J. Organomet. Chem.* **1978**, *162*, 189.

(4) Ungváry, F.; Markó, L. *J. Org. Chem.* **1969**, *20*, 205.

(5) See for instance: (a) Collman, J. P.; Hegedus, L. S.; Norton, J. R.; Finke, R. G. *Principles and Applications of Organotransition Metal Chemistry*; University Science Books: Mill Valley, CA, 1987. (b) Cotton, F. A.; Wilkinson, G. *Advanced Inorganic Chemistry*; Wiley: New York, 1988.

pioneering study of the hydroformylation reaction by Versluis, Ziegler, Baerends, and Ravenek (VZBR),⁹ the migration reactions for $\text{R} = \text{H}$ and $\text{R} = \text{CH}_3$ were studied using the Hartree–Fock–Slater¹¹ method. For $\text{R} = \text{CH}_3$, VZBR identified four conformers of $\text{CH}_3(\text{CO})\text{Co}(\text{CO})_3$ on the HFS potential energy surface. They predicted the most stable acyl species to be $(\eta^2\text{-CH}_3)(\text{CO})\text{Co}(\text{CO})_3$, with the acyl group occupying an equatorial site and the oxygen atom of the acyl group stabilizing the vacant axial site. A linear transit procedure¹² was used to approximate the energy profile for the migration process under a C_s symmetry constraint, and the activation energy was predicted to be 19.1 kcal/mol. In addition, they showed that the direct addition of CO to $\text{CH}_3\text{Co}(\text{CO})_4$ was likely to have a much larger activation barrier than the two-step migration/insertion reaction. While the work of VZBR suffers from some of the inevitable computational deficiencies of relatively early computational organometallic chemistry research (primarily the lack of characterization of stationary points and the imposition of symmetry), it has greatly contributed to the understanding of the catalytic cycle shown in Scheme 1.

In this paper, we extend our previous study¹³ on the migratory insertion of CO into pentacarbonyl(methyl)manganese(I) to the analogous cobalt system tetracarbonyl(methyl)cobalt(I). The main focus of our study is to identify the structures of the acyl intermediate, $\text{CH}_3(\text{CO})\text{Co}(\text{CO})_3$, and the various transition-state structures for intramolecular rearrangement and addition of CO. We demonstrate that, of the four coordinatively unsaturated acyl species previously considered,⁹ only two are minima on the B3LYP potential energy surface. The other species are saddle points corresponding to the rotation of the acyl group. We further show that, unlike the corresponding manganese system, methyl migration does not proceed along a path with C_s symmetry but, rather, involves a simultaneous migration and twisting of the axial methyl group in $\text{CH}_3\text{Co}(\text{CO})_4$ into the equatorial plane and subsequent relaxation to form an intermediate best described as an axially substituted

$\text{CH}_3(\text{CO})\text{Co}(\text{CO})_3$ species, with an agostic bond occupying the formally vacant equatorial site.

Computational Details

Theoretical treatment of first-row transition-metal systems is notoriously difficult because of the near-degeneracy of many of the electron configurations resulting from the partially filled 4s and 3d orbitals. To obtain quantitative results on these systems, a multireference method, such as multireference single and doubles configuration interaction (MR-SDCI),¹⁴ is in principle required. However, the computational effort for any type of MR method is prohibitively expensive for most organometallic species. Often, less expensive methods, such as second-order Møller–Plesset perturbation theory (MP2) or density functional theory (DFT), are used. However, it is well known that the MP2 method often leads to significant errors for first-row transition-metal systems.^{15,16} In contrast, there are several reports¹⁷ in the literature describing the satisfactory performance of hybrid density functional methods for these systems.

We employed the Becke three-parameter gradient-corrected hybrid exchange functional and the Lee–Yang–Parr correlation functional (B3LYP)¹⁸ in this study. The Gaussian 98 (G98) program package was used throughout.¹⁹ The Wachters-Hay²⁰ all-electron basis set (denoted 6-311+G in G98) was used for cobalt. The standard 6-31G**²¹ (5d) basis set was used for all other atoms.

All stationary points found on the potential energy surface were subsequently characterized by calculating frequencies analytically at the B3LYP level using the same basis set.

As we will see, the potential energy surface for $\text{CH}_3\text{Co}(\text{CO})_4$ alone has three minima and five transition states, and in many cases the relationships between the various stationary points are not entirely obvious. Because of the difficulties in properly connecting transition states to minima, the following procedure was employed for all transition states: (1) the transition state geometry was distorted along the normal mode corresponding to the imaginary frequency (in both directions, when appropriate) and (2) a full geometry optimization was subsequently performed, recalculating the analytic first and second derivatives at each step, until a minimum was reached.

- (6) (a) Grima, J. P.; Choplin, F.; Kaufmann, G. J. *J. Organomet. Chem.* **1977**, *129*, 221. (b) Fønnesbech, N.; Hjortkjær, J.; Johansen, H. *Int. J. Quantum Chem.* **1977**, *12*, 95. (c) Berke, H.; Hoffmann, R. *J. Am. Chem. Soc.* **1978**, *100*, 7224. (d) Pensak, D. A.; McKinney, R. J. *Inorg. Chem.* **1979**, *18*, 3407. (e) Eyer mann, C. J.; Chung-Phillips, A. *J. Am. Chem. Soc.* **1984**, *106*, 7437.
- (7) (a) Veillard, A.; Strich, A. *J. Am. Chem. Soc.* **1988**, *110*, 3793. (b) Daniel, C.; Hyla-Kryspin, I.; Demuyne, J.; Veillard, A. *Nouv. J. Chim.* **1985**, *9*, 581. (c) Veillard, A.; Daniel, C.; Rohmer, M. M. *J. Phys. Chem.* **1990**, *94*, 5556.
- (8) (a) Antolovic, D.; Davidson, E. R. *J. Am. Chem. Soc.* **1987**, *109*, 977. (b) Antolovic, D.; Davidson, E. R. *J. Am. Chem. Soc.* **1987**, *109*, 5828. (c) Antolovic, D.; Davidson, E. R. *J. Chem. Phys.* **1988**, *88*, 4967.
- (9) (a) Versluis, L.; Ziegler, T.; Baerends, E. J.; Ravenek, W. *J. Am. Chem. Soc.* **1989**, *111*, 2018. (b) Versluis, L.; Ziegler, T. *Organometallics* **1990**, *9*, 2985. (c) Versluis, L.; Ziegler, T. *Inorg. Chem.* **1990**, *29*, 4530. (d) Versluis, L.; Ziegler, T. *J. Am. Chem. Soc.* **1990**, *112*, 6763. (e) Ziegler, T. *Pure Appl. Chem.* **1991**, *63*, 873. (f) Ziegler, T.; Versluis, L. *Adv. Chem. Ser.* **1992**, No. 230, 75. (g) Ziegler, T.; Cavallo, L.; Bérces, A. *Organometallics* **1993**, *12*, 3586. (h) Miquel, S.; Ziegler, T. *Organometallics* **1996**, *15*, 2611.
- (10) Rogers, J. R.; Kwon, O.; Marynick, D. S. *Organometallics* **1991**, *10*, 2816.
- (11) Slater, J. C. *Adv. Quantum Chem.* **1972**, *6*, 1. Baerends, E. J.; Ellis, D. E.; Ros, P. *Chem. Phys.* **1973**, *2*, 41.
- (12) (a) Salem, L. In *Electrons in Chemical Reactions*; Wiley: New York, 1982. (b) Komornicki, A.; McIver, J. W. *J. Am. Chem. Soc.* **1974**, *96*, 5798.
- (13) Derecskei-Kovacs, A.; Marynick, D. S. *J. Am. Chem. Soc.* **2000**, *122*, 2078.

- (14) (a) Werner, H. J.; Knowles, P. J. *J. Chem. Phys.* **1985**, *82*, 5053. (b) Knowles, P. J.; Werner, H. J. *Chem. Phys. Lett.* **1985**, *115*, 259. (c) Werner, H. J.; Knowles, P. J. MOLPRO; University of Sussex, 1991.
- (15) Frenking, G.; Antes, I.; Boehme, M.; Dapprich, S.; Ehlers, A. W.; Jonas, V.; Nehaus, A.; Otto, M.; Stegmann, R.; Veldjamp, A.; Vydroshchikov, S. F. In *Reviews in Computational Chemistry*; Lipkowitz, K. B., Boyd, D. B., Eds.; VCH: New York, 1996; Vol. 8, p 63.
- (16) Torrent, M.; Gili, P.; Duran, M.; Solà, M. *J. Chem. Phys.* **1996**, *104*, 9499.
- (17) (a) Bauschlicher, C. W.; Ricca, A.; Partridge, H.; Langhoff, S. R. In *Recent Advances in Density Functional Theory*; Chong, D. P., Ed.; World Scientific: Singapore, 1997; Part II. (b) Siegbahn, P. E. M. Electronic Calculations for Molecules Containing Transition Metals. *Adv. Chem. Phys.* **1996**, XCIII. (c) Pavlov, M.; Siegbahn, P. E. M.; Sandström, M. *J. Phys. Chem. A* **1998**, *102*, 219. (d) Filatov, M.; Shaik, S. *J. Phys. Chem. A* **1998**, *102*, 3835.
- (18) (a) Becke, A. D. *J. Chem. Phys.* **1993**, *98*, 5648. (b) Lee, C.; Yang, W.; Parr, R. G. *Phys. Rev. B* **1988**, *37*, 785.
- (19) Frisch, M. J.; Trucks, G. W.; Schlegel, H. B.; Scuseria, G. E.; Robb, M. A.; Cheeseman, J. R.; Zakrzewski, V. G.; Montgomery, J. A., Jr.; Stratmann, R. E.; Burant, J. C.; Dapprich, S.; Millam, J. M.; Daniels, A. D.; Kudin, K. N.; Strain, M. C.; Farkas, O.; Tomasi, J.; Barone, V.; Cossi, M.; Cammi, R.; Mennucci, B.; Pomelli, C.; Adamo, C.; Clifford, S.; Ochterski, J.; Petersson, G. A.; Ayala, P. Y.; Cui, Q.; Morokuma, K.; Malick, D. K.; Rabuck, A. D.; Raghavachari, K.; Foresman, J. B.; Cioslowski, J.; Ortiz, J. V.; Stefanov, B. B.; Liu, G.; Liashenko, A.; Piskorz, P.; Komaromi, I.; Gomperts, R.; Martin, R. L.; Fox, D. J.; Keith, T.; Al-Laham, M. A.; Peng, C. Y.; Nanayakkara, A.; Gonzalez, C.; Challacombe, M.; Gill, P. M. W.; Johnson, B. G.; Chen, W.; Wong, M. W.; Andres, J. L.; Head-Gordon, M.; Replogle, E. S.; Pople, J. A. *Gaussian 98*, revision A.1; Gaussian, Inc.: Pittsburgh, PA, 1998.
- (20) (a) Wachters, A. J. H. *J. Chem. Phys.* **1970**, *52*, 1033. (b) Hay, P. J. *J. Chem. Phys.* **1977**, *66*, 4377.
- (21) Hariharan, P. C.; Pople, J. A. *Theor. Chim. Acta* **1973**, *28*, 213.

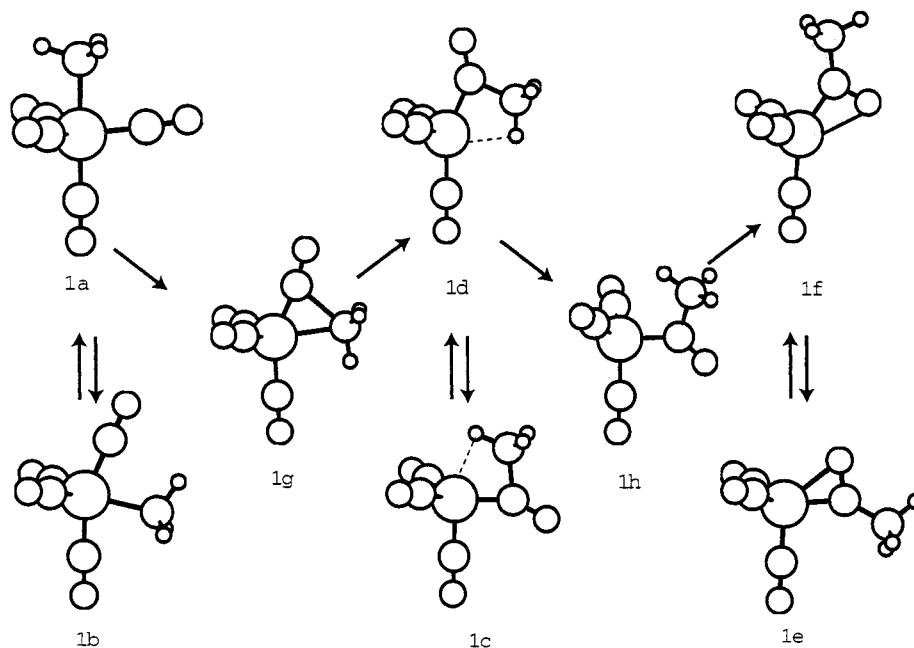


Figure 1. Stationary points on the tetracarbonyl(methyl)cobalt(I) potential energy surface and their interrelationships. Structures **1a**, **1d**, and **1f** are minima. All other structures are transition states.

Result and Discussion

CH₃Co(CO)₄. Figure 1 shows all of the stationary points on the potential energy surface of CH₃Co(CO)₄. Let us first focus on the trigonal-bipyramidal reactant **1a**, with the methyl group in the axial position and C_{3v} symmetry, and the closely related structure **1b**, with the methyl group in the equatorial position and C_s symmetry. Only **1a** is a true minimum on the potential energy surface. The molecular structure of CH₃Co(CO)₄ is not known experimentally. However, a matrix-isolation study by Sweany and Russell²² strongly suggests that CH₃Co(CO)₄ has C_{3v} symmetry with an axial methyl group. This is in accord with the observation that a strong σ donor ligand, such as a methyl group, forms a stronger bond to the axial position than the to the equatorial position for d⁸ systems.²³ **1b** is found to be a transition state with a single imaginary frequency of 76i cm⁻¹. Relaxation of the transition state geometry along the imaginary vibrational mode as described in Computational Details demonstrates that **1b** is a transition state for the pseudorotation of two equivalent forms of **1a**. The barrier for pseudorotation is found to be 9.5 kcal/mol.

CH₃(CO)Co(CO)₃ Stationary Points. Migratory insertion can presumably proceed via the following two pathways: (1) migration of the CH₃ group to a cis carbonyl and (2) insertion of a cis carbonyl into the CH₃-CO bond. A thorough search of the potential energy surface yielded six stationary points in addition to the two discussed above: two minima and four first-order saddle points. All eight stationary points are shown in Figure 1, as is the relationship between the various minima and saddle points. The energetics are summarized in Table 1.²⁴ Structures **1d** and **1f** are minima, and both may be thought of as distorted trigonal bipyramids with the acyl carbons in the axial

Table 1. Relative Energies of the Species Involved in the First Step of the Carbonylation of CH₃(CO)Co(CO)₄^a

	structure	rel energy (kcal/mol)
reactant	1a	0.0
transition state	1b	9.5
transition state	1g	12.0
intermediate	1d	6.5
transition state	1c	13.3
transition state	1h	15.9
intermediate	1f	2.7
transition state	1e	6.7

^a Zero-point energy corrections at the B3LYP level are included. For the saddle points, the imaginary frequencies are 77i (**1b**), 248i (**1g**), 75i (**1c**), 201i (**1h**), and 66i (**1e**).

position, as would be expected from σ bonding considerations.²³ **1d** can be considered a 16-electron trigonal bipyramid with an axial acyl group and an agostic bond to the formally vacant equatorial Co site. **1f** may be thought of as an 18-electron, severely distorted, trigonal bipyramid with the acyl carbon in the axial position and the acyl oxygen occupying the equatorial position.

The first step in the migration process is the formation of **1d** from **1a** via the transition state **1g**. The overall step is endoergic by 6.5 kcal/mol, with a barrier of 12.0 kcal/mol. While the process **1g** \rightarrow **1d** is easy to visualize, the step **1a** \rightarrow **1g** is not. The entire sequence is presented in Figure 2, which clearly shows that as

(24) For comparison, we have also calculated the energetics of all structures at the BP86 level using the B3LYP geometries (BP86//B3LYP). The calculated energetics (in kcal/mol, without ZPE corrections) are as follows: **1a** (0.0), **1b** (8.4), **1c** (8.8), **1d** (3.3), **1e** (5.3), **1f** (1.0), **1g** (9.9), **1h** (13.7), **2a** (6.3), **2b** (10.8), **2c** (1.1), **2d** (8.3) and **2e** (-23.0). Excluding **2e**, the two approaches agree to within an average absolute error of 2.0 kcal/mol. However, BP86 predicts the ΔE of the overall carbonylation reaction (which corresponds to the energy of **2e**) to be 9.2 kcal/mol more exoergic than B3LYP. While the experimental value is not known, our earlier study of the carbonylation of pentacarbonyl(methyl)manganese(I) showed very similar behavior. In that case, the experimental value was known, and the calculated value using the B3LYP functional was in much better agreement with experiment. For this reason, we have used the B3LYP energetics as the basis of the mechanistic discussions in what follows.

(22) Sweany, R. L.; Russell, F. N. *Organometallics* **1988**, *7*, 719.

(23) Rossi, A. R.; Hoffmann, R. *Inorg. Chem.* **1975**, *14*, 365.

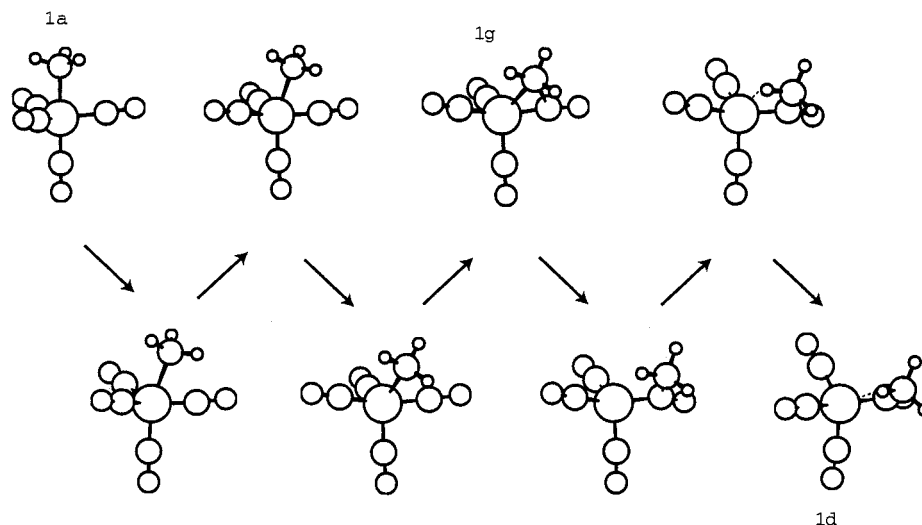


Figure 2. Details of the migration/twist step interconnecting **1a** to **1d** through transition state **1g**.

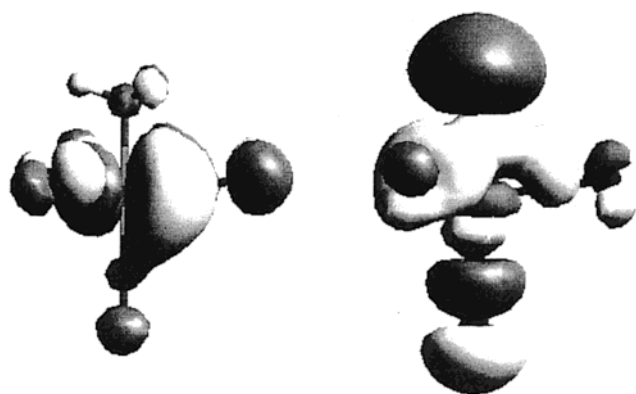


Figure 3. HOMO (left) and LUMO (right) of $\text{CH}_3\text{Co}(\text{CO})_5$.

the CH_3 group gradually migrates to the cis CO, it simultaneously rotates toward the equatorial plane. This motion is qualitatively different than we¹⁰ and others⁹ have previously assumed, in that C_s symmetry is not preserved.²⁵ The origin of this unusual migration/twist mechanism is easy to understand by examining the frontier orbitals of **1a** (see Figure 3). The HOMO has e symmetry and lies dominantly in the equatorial plane of the molecule. The LUMO has a_1 symmetry and lies along the C_3 axis. Efficient mixing of these two orbitals can only be achieved by twisting the CH_3 group toward the equatorial position as the migration proceeds.²⁶

1d may further react by forming the η^2 stabilized structure **1f**. Structure **1h**, the transition state for this process, may be described as a distorted tetrahedron with an η^1 acyl group. The process **1d** \rightarrow **1f** is exoergic by 3.8 kcal/mol, with an activation energy of 9.4 kcal/mol. Again, the relationship between **1d** and **1h** is not entirely obvious without a detailed search of the potential energy surface. In Figure 4, we present the key structures connecting **1d** and **1f** through the transition state structure **1h**. The **1d** \rightarrow **1h** process is dominantly

a rotation of the acyl group by $\sim 60^\circ$ with a concurrent opening up of the $\text{Co}-\text{C}_{\text{acyl}}-\text{C}_{\text{methyl}}$ angle. Relaxation of **1h** to **1f** is accomplished by a rotation of the methyl group by $\sim 60^\circ$ followed by a reduction of the $\text{Co}-\text{C}_{\text{acyl}}-\text{O}$ angle to yield the η^2 stabilized intermediate.

Thus far, we have illustrated that reactant **1a** proceeds to the agostic form **1d** via a migration/twist of the CH_3 group and that **1d** can subsequently rearrange to the slightly more stable η^2 form **1f** with a very modest activation energy. In principle, however, the η^2 intermediate **1f** could also be obtained by a direct insertion of an equatorial CO ligand into the $\text{Co}-\text{CH}_3$ bond, i.e., **1a** \rightarrow **1f**. However, numerous attempts to locate a transition state between these structures were not successful. Thus, it is very likely that no low-energy transition state structure connects **1a** to **1f** and that a direct insertion of a CO ligand into a $\text{Co}-\text{CH}_3$ bond is not feasible. This finding is in general accord with a large body of evidence on other metal systems suggesting that alkyl group migration is generally preferred over CO insertion.⁵ In addition, our results are consistent with labeling experiments on an analogous system ($\text{PhCH}_2-\text{Co}(\text{CO})_3\text{PPh}_3$),²⁷ which suggested that alkyl migration was the dominate mechanism for this species, and with previous theoretical work.⁹

Two remaining stationary points on the potential energy surface of $\text{CH}_3\text{Co}(\text{CO})_4$ remain to be discussed. Both **1c** and **1e** have acyl group carbons in the equatorial positions of distorted trigonal bipyramids, and both represent first-order saddle points. **1c** is found to be the transition state for acyl group rotation connecting two **1d** minima. The barrier for the acyl rotation is 6.8 kcal/mol. Similarly, **1e** corresponds to the transition state for acyl rotation connecting two η^2 acyl intermediates. The barrier for this rotation is found to be 4.0 kcal/mol. Our results demonstrate that structures **1b**, **1c**, and **1e** are all transition states for ancillary rotation/pseudorotation processes but do not play a significant role in the migration/insertion process.

Carbonylation of $\text{CH}_3(\text{CO})\text{Co}(\text{CO})_3$. In the presence of excess CO, $\text{CH}_3(\text{CO})\text{Co}(\text{CO})_3$ readily reacts with CO to form a stable 18-electron product, $\text{CH}_3(\text{CO})\text{Co}-$

(25) A similar motion has been shown to be operative in the related systems $\text{Rh}(\text{H})(\text{C}_2\text{H}_4)(\text{CO})_2(\text{PH}_3)$ and $\text{Rh}(\text{H})(\text{CO})_2(\text{PH}_3)_2$. See: Koga, N.; Jin, S. Q.; Morokuma, K. *J. Am. Chem. Soc.* **1988**, *110*, 3417. Matsubara, T.; Koga, N.; Ding, J.; Musaev, D. G.; Morokuma, K. *Organometallics* **1997**, *16*, 1065.

(26) These plots were obtained with Spartan 5.0 (Wavefunction, Inc., Irving, CA).

(27) Nagy-Magos, Z.; Bor, G.; Markó, L. *J. Organomet. Chem.* **1968**, *14*, 205.

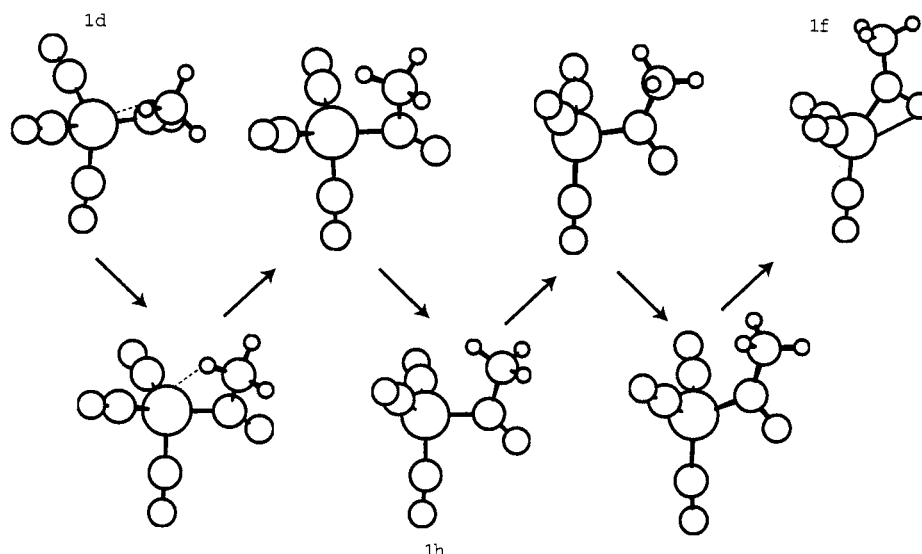


Figure 4. Details of the step **1d** to **1f** through the transition state **1h**.

Table 2. Relative Energies of the Species Involved in the Second Step of the Carbonylation of $\text{CH}_3(\text{CO})\text{Co}(\text{CO})_4$ ^a

	structure	rel energy (kcal/mol)
transition state	2a	8.1
transition state	2b	8.2
transition state	2c	2.8
transition state	2d	8.2
product	2e	-13.8

^a Relative to $\text{CH}_3\text{Co}(\text{CO})_4$ + free CO. Zero-point energy corrections at the B3LYP level are included. The imaginary frequencies are 91*i* (**2a**), 44*i* (**2b**), 101*i* (**2c**), and 136*i* (**2d**).

(CO)₄. There are two possible channels for the coordination of carbonyl to the acyl species $\text{CH}_3(\text{CO})\text{Co}(\text{CO})_3$: (1) the incoming CO attacks the agostic acyl species **1d** and (2) the agostic acyl species rearranges to the more stable η^2 form **1f**, followed by CO attack. Both reaction channels yield the same overall products. The energies of all relevant stationary points for these processes, relative to the sum of the energy of the reactant and free carbon monoxide, are listed in Table 2.

First consider the reaction **1d** + CO → $\text{CH}_3(\text{CO})\text{Co}(\text{CO})_4$. Two transition state structures (**2a** and **2b** in Figure 5) were found. Structures **2a** and **2b** represent the attack of CO from the front and back sides of the agostic bond, respectively. Both reactions have extremely low activation energies: 1.6 kcal/mol for **2a** and 1.7 kcal/mol for **2b**.

Similarly, we located two transition state structures, **2c** and **2d**, for the reaction **1f** + CO → $\text{CH}_3(\text{CO})\text{Co}(\text{CO})_4$. Attack of CO from the oxygen side of the acyl group through transition state **2c** is a nearly barrierless process ($E_a = 0.1$ kcal/mol), while CO attack from the other side proceeds with an activation energy of 5.5 kcal/mol. We conclude that CO attack on **1f** would proceed through transition state **2c**. The higher energy of **2d** is easily understood by comparing the structure of **1f** with those of **2c** and **2d**: the $\text{CH}_3(\text{CO})\text{Co}(\text{CO})_3$ unit of **2c** is considerably less distorted than that of **2d**.

What is the dominant mechanism for CO addition in this system? Since the activation energies for the bimolecular addition of CO to **1d** and **1f** are both very small, the energetics of intramolecular rearrangement become of crucial importance. The important activation

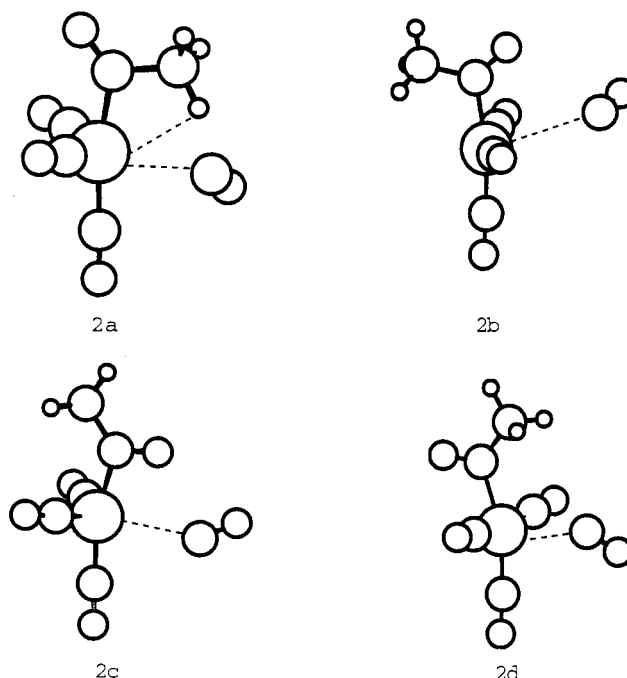
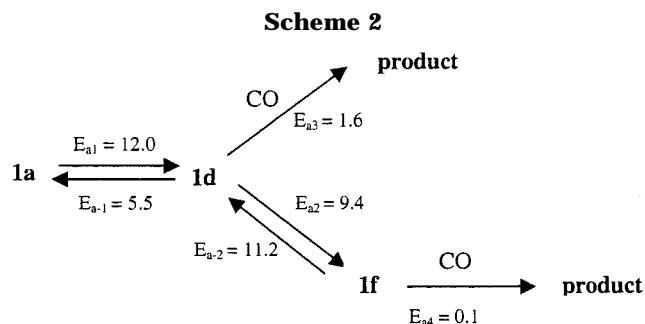


Figure 5. Transition states for attack of CO on structure **1d** (**2a** and **2b**) and on structure **1f** (**2c** and **2d**).



energies are summarized in Scheme 2. Although the mechanistic details of the carbonylation reactions of $\text{CH}_3\text{Mn}(\text{CO})_5$ and $\text{CH}_3\text{Co}(\text{CO})_4$ are significantly different (all of the relevant stationary points and reactions pathways lie essentially on a C_s potential energy surface for the manganese systems while, as we have seen, this

is distinctly not the case for the cobalt system), the main features of the two systems are quite similar. Both display agostic and η^2 stabilized intermediates, both have a coordinatively unsaturated $16e^-$ species with an η^1 acyl group as the transition state between these two intermediates, and the shapes of the potential energy surfaces are qualitatively similar. For $(\text{CH}_3)\text{Mn}(\text{CO})_5$, we showed,¹³ using a kinetic model constructed from our DFT energetics, experimental kinetics observations, and estimates of preexponential factors for key elementary steps, that carbonylation most likely occurs by attack of the agostically stabilized intermediate, even though the η^2 stabilized intermediate is lower in energy. No such conclusion can be drawn here. Assuming Arrhenius behavior for all steps, and the calculated activation energies in Scheme 1, we need only estimate the preexponential factors (A) of the various steps to determine the dominant reaction pathway. While the preexponential factors are not known, we previously estimated¹³ the ratio of bimolecular to unimolecular preexponential factors for the manganese system at 10^{-2} mol mL^{-1} . This estimate was based on a range of gas-phase unimolecular and bimolecular reactions and can be rationalized on the basis of frequencies for simple bond stretches and collision frequencies.²⁸ Additionally, the solubility of CO in a variety of solvents is in the range of 10^{-5} – 10^{-6} mol mL^{-1} .^{13,29} Assuming $[\text{CO}] = 5 \times 10^{-6}$ mol mL^{-1} , $[\mathbf{1a}] = 1.0 \times 10^{-4}$ mol mL^{-1} , and $A(\text{bimol})/A(\text{unimol}) = 10^{-2}$ mol mL^{-1} , the rate equations implicit in Scheme 2 can be numerically integrated. We find that the reaction proceeds only 3% via channel 1 and 97% via channel 2. This result can be understood as follows. Since both channels must proceed through the intermediate $\mathbf{1d}$, first consider the relative rates of the carbonylation of $\mathbf{1d}$ and the interconversion of $\mathbf{1d}$ to $\mathbf{1f}$. At 298 K

$$\frac{\text{rate}(\mathbf{1d} + \text{CO} \rightarrow \text{product})}{\text{rate}(\mathbf{1d} \rightarrow \mathbf{1f})} = \frac{k_3[\mathbf{1d}][\text{CO}]}{k_2[\mathbf{1d}]} = \frac{A_3 e^{-E_{a3}/RT}[\text{CO}]}{A_2 e^{-E_{a2}/RT}} = \frac{A(\text{bimol}) e^{-E_{a3}/RT}[\text{CO}]}{A(\text{unimol}) e^{-E_{a2}/RT}} = 0.03$$

Thus, $\sim 97\%$ of $\mathbf{1d}$ is converted to $\mathbf{1f}$. Now consider the relative rates of the carbonylation of $\mathbf{1f}$ and the interconversion of $\mathbf{1f}$ to $\mathbf{1d}$:

$$\frac{\text{rate}(\mathbf{1f} + \text{CO} \rightarrow \text{product})}{\text{rate}(\mathbf{1f} \rightarrow \mathbf{1d})} = \frac{k_4[\mathbf{1f}][\text{CO}]}{k_{-2}[\mathbf{1f}]} = \frac{A_4 e^{-E_{a4}/RT}[\text{CO}]}{A_{-2} e^{-E_{a-2}/RT}} = \frac{A(\text{bimol}) e^{-E_{a4}/RT}[\text{CO}]}{A(\text{unimol}) e^{-E_{a-2}/RT}} = 200$$

Therefore, almost all of $\mathbf{1f}$ undergoes carbonylation (as opposed to back-reacting to form $\mathbf{1d}$). Of course, given the nature of our assumptions concerning the relative magnitude of the various preexponential terms and the uncertainty of the accuracy of the calculated potential energy surface, we cannot make a definitive conclusion

as to the dominance of one channel over the other. However, we can conclude that the two channels are likely to be competitive, and the dominant channel will probably depend on the conditions of the reaction (solvent, temperature, etc.).

Summary and Conclusions

The migratory insertion of a methyl group into the Co–CO bond (step 4 of the hydroformylation process of Scheme 1) and the coordination of CO to $\text{CH}_3(\text{CO})\text{Co}(\text{CO})_3$ were studied using gradient-corrected density functional techniques with reasonably large basis sets.

The reactant $\text{CH}_3\text{Co}(\text{CO})_4$ was found to be a trigonal bipyramid with C_{3v} symmetry, in agreement with a matrix-isolation study and simple qualitative bonding arguments. A second trigonal bipyramid, with the methyl group in the equatorial position, was found to be the transition state for pseudorotation of the reactant. Of the four possible structures for the intermediate $\text{CH}_3(\text{CO})\text{Co}(\text{CO})_3$ considered, only $\mathbf{1d}$ and $\mathbf{1f}$ are found to be true minima on the potential energy surface. Structures $\mathbf{1c}$ and $\mathbf{1e}$ are found to be transition states corresponding to the rotation of the acyl groups. A interesting feature of this reaction, and one not heretofore appreciated, is that alkyl group migration is accompanied by a simultaneous twist of the alkyl group into the equatorial plane of the original trigonal bipyramid. The driving force for this migration/twist process is HOMO/LUMO mixing: the LUMO, predominantly of Co–CH₃ character and lying along the major rotation axis of the molecule, must twist into the equatorial plane to mix with one of the components of the HOMO, of e symmetry. In contrast, no such twisting is required in the prototypical model for alkyl group migration, pentacarbonyl(methyl)manganese(I).³⁰

We also investigated two reaction channels for the thermal carbonylation of tetracarbonyl(methyl)cobalt. Both channels follow a multistep mechanism. In channel 1, the reactant proceeds to the agostic form $\mathbf{1d}$ followed by the CO attack. In the second reaction channel, the agostic structure $\mathbf{1d}$ rearranged to the more stable η^2 species $\mathbf{1f}$ followed by CO attack. Simple kinetic arguments suggest that the two channels are competitive.

Acknowledgment. We thank the Welch Foundation (Grant No. Y-0743) for support of this research.

Supporting Information Available: Tables giving Cartesian coordinates and energies for all stationary points. This material is available free of charge via the Internet at <http://pubs.acs.org>.

OM0200297

(28) DeMore, W. B.; Sander, S. P.; Howard, C. J.; Ravinshankara, A. R.; Golden, D. M.; Kolb, C. E.; Hampson, R. F.; Kurylo, M. J.; Molina, M. J. *Chemical Kinetics and Photochemical Data for Use in Stratospheric Modeling*; Evaluation Number 12, Jet Propulsion Laboratory, 1997.

(29) Gerrard, W. *Solubility of Gases and Liquids*; Plenum Press: New York, London, 1976.

(30) In $\text{CH}_3\text{Mn}(\text{CO})_5$, the lowest three LUMOs have dominant contributions from carbonyl π^* orbitals and are essentially degenerate. One of these orbitals is dominated by carbonyl π^* 's cis to, and in the same plane as, the methyl group. Migration of the methyl group to a cis CO is therefore easily achieved without breaking symmetry by mixing of the Mn–CH₃ bonding orbital with the appropriate in-plane LUMO.